Journal of Nuclear Medicine, published on July 6, 2023 as doi:10.2967/jnumed.122.264770

Dual-Time-Point Posttherapy ^{177}Lu-PSMA-617 SPECT/CT Describes the Uptake Kinetics of mCRPC Lesions and Prognosticates Patients' Outcome

Manuela Straub[1], Jürgen Kupferschläger[1], Lina Maria Serna Higuita[2], Matthias Weissinger[1,3], Helmut Dittmann[1], Christian la Fougère[1,4,5], and Francesco Fiz[1,6]

[1]*Department of Nuclear Medicine and Clinical Molecular Imaging, University Hospital, Tübingen, Germany;* [2]*Institute of Clinical Epidemiology and Applied Biometry, University of Tübingen, Tübingen, Germany;* [3]*Department of Radiology, University Hospital, Tübingen, Germany;* [4]*Cluster of Excellence 2180 "Image-Guided and Functionally Instructed Tumor Therapies," Eberhard Karls University, Tübingen, Germany;* [5]*German Cancer Consortium, German Cancer Research Center Partner Site Tübingen, Tübingen, Germany; and* [6]*Nuclear Medicine Unit, Department of Diagnostic Imaging, Ente Ospedaliero "Ospedali Galliera," Genoa, Italy*

^{177}Lu-PSMA-617 is an effective therapeutic option in metastasized castration-resistant prostate cancer (mCRPC). However, some patients progress under treatment. We hypothesized that the tracer kinetics within the metastases may influence the therapy effectiveness and tested this hypothesis by analyzing uptake parameters on 2 consecutive posttherapy SPECT/CT scans. **Methods:** mCRPC patients treated with ^{177}Lu-PSMA-617 and with available posttherapy SPECT/CT imaging (24 and 48 h after the first treatment) were enrolled retrospectively. Volumes of interest were defined on lymph node metastasis (LNM) and bone metastasis (BM) on both SPECT/CT scans. The reduction of the percentage injected dose (%IDred) between the 2 SPECT/CT scans was computed. We compared %IDred of responders (prostate-specific antigen drop $\geq$ 50% after 2 cycles of ^{177}Lu-PSMA-617) and nonresponders. We tested the association of %IDred with progression-free survival and overall survival (OS) using a univariate Kaplan–Meier (KM) analysis and a multivariate Cox regression model. **Results:** Fifty-five patients (median age, 73 y; range, 54–87 y) were included. %IDred in LNM and BM was greater in nonresponders than in responders (for LNM, 36% in nonresponders [interquartile range (IQR), 26%–47%] vs. 24% in responders [IQR, 12%–33%] [$P = 0.003$]; for BM, 35% in nonresponders [IQR, 27%–52%] vs. 18% in responders [IQR, 15%–29%] [$P = 0.002$]). For progression-free survival, in KM analysis, greater %IDred in LNM ($P = 0.008$) and BM ($P = 0.001$) was associated with shorter survival, whereas in multivariate analysis, only %IDred in LNM was retained ($P = 0.03$). In univariate KM analysis of OS, greater %IDred in BM was associated with shorter survival ($P = 0.002$). In multivariate OS analysis, BM %IDred ($P = 0.009$) was retained. **Conclusion:** The ^{177}Lu-PSMA-617 clearance rate from mCRPC metastases appears to be a relevant prognosticator of response and survival, with faster clearing possibly signaling a shorter radiopharmaceutical residence time and absorbed dose. Dual-time-point analysis appears to be a feasible and readily available approach to estimate the likelihood of response and patients' survival.

Key Words: ^{177}Lu-PSMA-617; RLT; SPECT/CT; mCRPC; dual time point

J Nucl Med 2023; 00:1–8
DOI: 10.2967/jnumed.122.264770

Lutetium-177-PSMA-617 radioligand therapy (RLT) is a treatment option for prostate-specific membrane antigen (PSMA)–positive metastasized castration-resistant prostate cancer (mCRPC), which showed a survival rate superior to supportive treatment and a higher response rate with fewer adverse events than second-line chemotherapy (*1,2*). This treatment can induce a satisfactory response (prostate-specific antigen [PSA] decrease $>$ 50%) in more than half of the treated subjects and hinder progression in 30% of them (*2–6*). It is safe and well tolerated, with toxicity-related discontinuation being rare (*7*).

However, some patients progress during the treatment, despite having shown adequate PSMA uptake on the pretherapy PET (*8*), which should have implied adequate radiopharmaceutical binding and tumor radiation exposure. Nonetheless, the tumor dose depends on the area under the curve of uptake intensity and ^{177}Lu-PSMA-617 residence time within the lesions; those with a fast radiopharmaceutical turnover could therefore receive an insufficient radiation dose. Moreover, the ^{177}Lu-PSMA-617 kinetics could vary across metastasis types (lymph node metastasis [LNM], bone metastasis [BM], and organ metastasis localizations). Estimating the radiopharmaceutical residence time from PET images, using multiple acquisitions, is hardly feasible, given the short half-life of the current diagnostic radionuclides ^{68}Ga and ^{18}F. In opposition, this parameter could be estimated on the post-RLT scans using the γ-radiation component of ^{177}Lu-PSMA-617 (*9*).

A recent study confirmed that the dose to the metastases is pivotal in inducing response: patients receiving less than 10 Gy to the tumor localizations were unlikely to achieve a response (*10*). A full dosimetry approach is time-consuming and requires the patients to undergo a series of diagnostic acquisitions up to 7 d after ^{177}Lu-PSMA-617 administration (*10*). Therefore, it is not yet used in the clinical routine. However, in theory, the PSMA kinetics within the lesions could be estimated with as few as 2 imaging time points, which may allow identification of the rate of change between the scans. In this study, we measured the percentage injected dose (%ID) within the mCRPC secondary lesions on 2 posttherapy SPECT/CT scans; the objective was to test whether the percentual change of this parameter correlates with the patients' response, as well as with progression-free survival (PFS) and overall survival (OS).

Received Aug. 7, 2022; revision accepted Apr. 20, 2023.
For correspondence or reprints, contact Christian la Fougère (christian.lafougere@med.uni-tuebingen.de).
Published online Jul. 6, 2023.

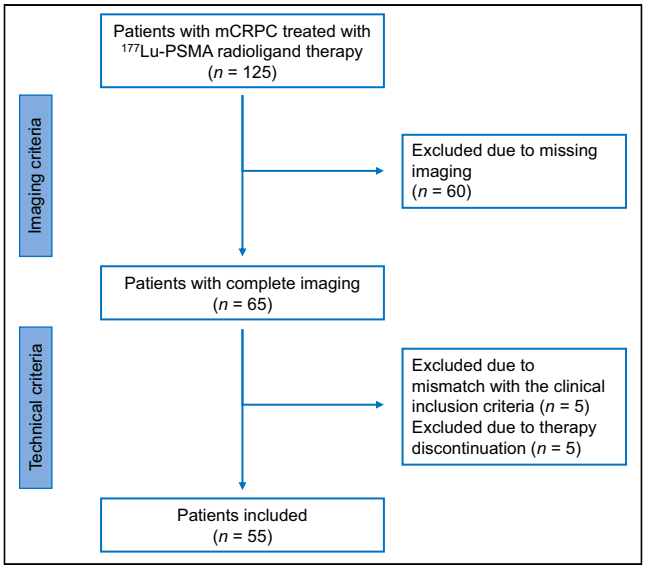

FIGURE 1. Patient recruitment workflow.

MATERIALS AND METHODS

Patients and Ethics

The local database was retrospectively searched for mCRPC patients treated with ^{177}Lu-PSMA-617 between April 2016 and September 2020. Criteria of eligibility for the treatment were histologically confirmed prostate cancer with progression to mCRPC status, adequate PSMA expression on a recent (<60 d) PET scan (^{18}F-PSMA-1007 or ^{68}Ga-PSMA-11), and approval by a registered multidisciplinary tumor board. Criteria of inclusion in the study were availability of dual-time-point SPECT/CT imaging (24 and 48 h after injection) at the time of the first RLT and at least 2 cycles of ^{177}Lu-PSMA-617. There was no set maximum number of RLT cycles; treatment was carried on until complete response, disease progression, or intolerable therapy-related toxicity.

Exclusion criteria were unavailability or insufficient quality of SPECT/CT imaging, neuroendocrine histology, presence of PSMA-negative or ^{18}F-FDG–positive disease (*11*), and later onset of PSMA-negative progression. Approval for this retrospective study was obtained from the local ethics committee of the University Hospital of Tübingen (decision 672/2019BO2), and the need to obtain specific consent was waived.

TABLE 1
Patient Population

Variable	All patients	Responders	Nonresponders*	$P^{\dagger}$
n	55	25	30	—
Age (y)	73 (67–79)	72 (74–76)	73 (64–79)	0.26
PSA	84 (22–307)	55 (19–146)	205 (30–565)	0.077
Hemoglobin (g/dL)	11 (10.1–12.1)	11.5 (10.6–13.1)	10.4 (10–11.4)	0.069
ANC (tsd/μL)	3.7 (3.2–4.8)	3.5 (2.7–4.4)	3.9 (3.2–4.8)	0.169
Platelets (tsd/μL)	233 (153–260)	209 (158–240)	236 (156–309)	0.098
Previous chemotherapy				
Yes	34 (62%)	15 (60%)	19 (63%)	0.927
No	21 (38%)	10 (40%)	11 (37%)	
Previous $^{223}RaCl_2$ (Xofigo; Bayer)				
Yes	7 (13%)	4 (16%)	3 (10%)	0.506
No	48 (87%)	21 (84%)	27 (90%)	
Previous treatments	3 (0–6)	3 (0–6)	3 (0–6)	0.93
PSMA cycles	3 (2–8)	4 (2–8)	2 (2–6)	0.006
Metastases				
LNM	43 (78%)	21 (84%)	22 (73%)	0.34
BM	43 (78%)	16 (64%)	27 (90%)	0.02
Organ	14 (26%)	6 (24%)	8 (27%)	0.82
Tumor volume (mL)				
LNM	25 (9.14–67.8)	27 (11.1–94.3)	19.7 (6.9–53.2)	0.62
BM	237 (58.9–525.8)	145 (50.5–569.7)	248.9 (81.8–489)	0.94
Organ	34 (9.82–52.7)	32.8 (15.5–38.1)	42 (7.9–56.9)	0.51

*This group includes both nonresponders and partial responders.
†Obtained by different statistical tests (see Materials and Methods).
ANC = absolute neutrophil count; tsd = thousand.
Continuous data are median and range; qualitative data are number and percentage.

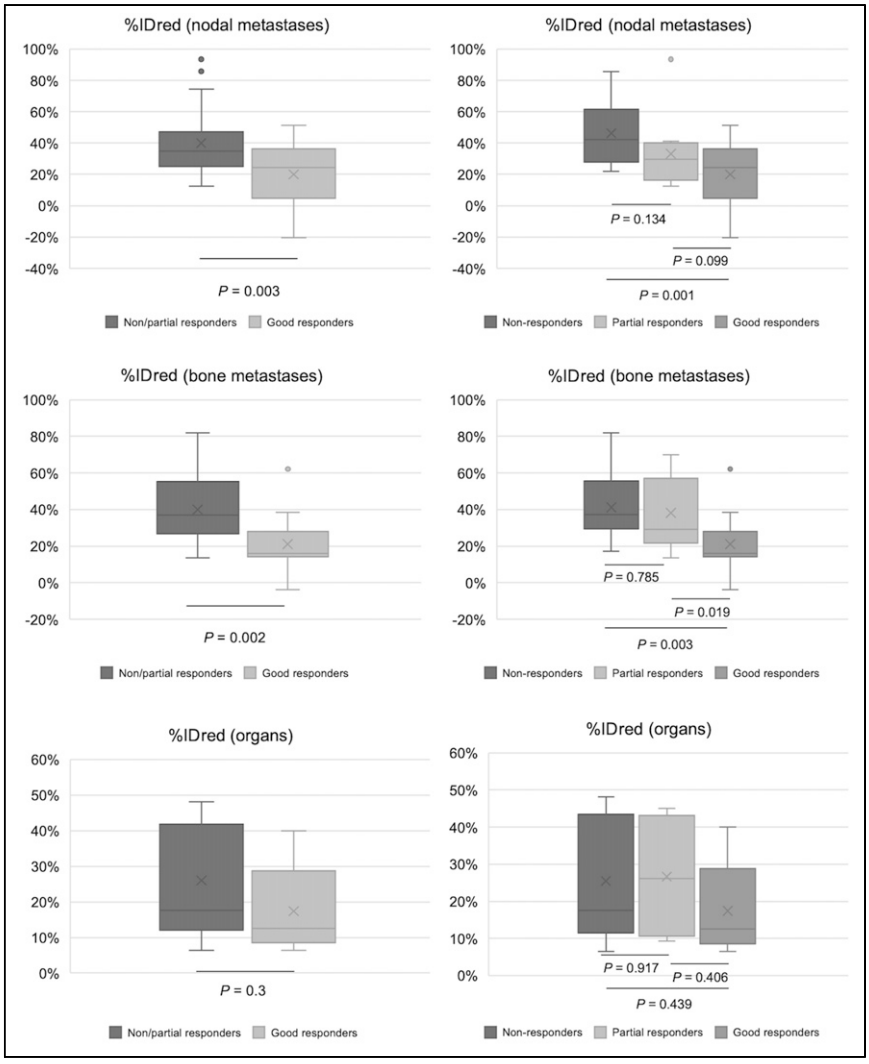

FIGURE 2. Median values of %IDred in LNM (top panels), BM (middle panels), and organ metastasis (bottom panels). Negative values represent increase in activity.

^{177}Lu-PSMA-617 SPECT/CT Acquisition and Reconstruction

Images were acquired 24 and 48 h after ^{177}Lu-PSMA-617 administration on a hybrid, dual-head γ-camera (NM/CT 670pro; GE Healthcare) equipped with medium-energy collimators. Whole-body planar acquisition (bed speed, 20 cm/min) and 2 or 3 SPECT/CT scans, to cover the field of view between the vertex and the mid thigh, were acquired. SPECT data (obtained with a 180° range, 6° steps, and a step time of 20 s) were reconstructed using a 3-dimensional, ordered-subset expectation maximization algorithm (with CT-based attenuation correction, scatter correction, and resolution recovery). CT had low-dose settings (30 mA, 120 kV). The SPECT and CT images were then coregistered (Xeleris V.4; GE Healthcare).

Image Analysis

SPECT/CT images acquired after the first ^{177}Lu-PSMA-617 administration were analyzed using a commercial application (Volumetrix MI; GE Healthcare). On loading the first SPECT/CT scan, the injected and residual activity, as well as calibration and administration times, were inserted. Volumes of interest (VOIs) were constructed semiautomatically on the LNM, BM, and organ metastasis localization by first encasing the target lesions in a large VOI and then applying automatic thresholding (41% of the maximum voxel value); finally, nontarget areas were manually excluded. The minimum VOI was set at 5 cm^3. The sum of all VOIs was labeled tumor burden.

For each VOI, the system calculated the mean and maximum activity concentrations and %ID (that is, the percentage of the initial injected dose that was retained within a specific volume in the 2 time points). We computed this parameter for the LNM, BM, and organ metastasis localizations separately, as well as a single score including all disease localizations (%ID total). For the main purposes of our analysis, we considered this last parameter only because of its robustness (*12*). Concentration indices were tested only in the differentiation between responders and nonresponders; we did not compute weight-normalized indices, such as SUV_{mean} or SUV_{max}, because they can underperform in the evaluation of tissue-specific tracers (*13*). All VOIs were then exported onto the second dataset, and positioning adjustments were made whenever necessary. Finally, we calculated the relative reduction of %ID (%IDred) from the first to the second SPECT/CT scan in each district (LNM, BM, and organ metastasis).

Study Objectives

The first objective was to test whether there are differences in %IDred between responders (PSA drop ≥ 50% after 2 RLTs) and nonresponders. In a subanalysis, patients were stratified into good responders (PSA drop ≥ 50%), partial responders (PSA drop, 1%–50%), and nonresponders (no PSA drop or progression). The PSA variation was calculated as the percent difference between the baseline value (on the day of the first RLT, before ^{177}Lu-PSMA-617 administration) and the measurement 1 mo after the second RLT cycle.

The second objective was to identify whether %IDred or baseline %ID in any of the considered disease localizations correlated with PFS or OS. All patients had routinely undergone a clinical or laboratory data evaluation

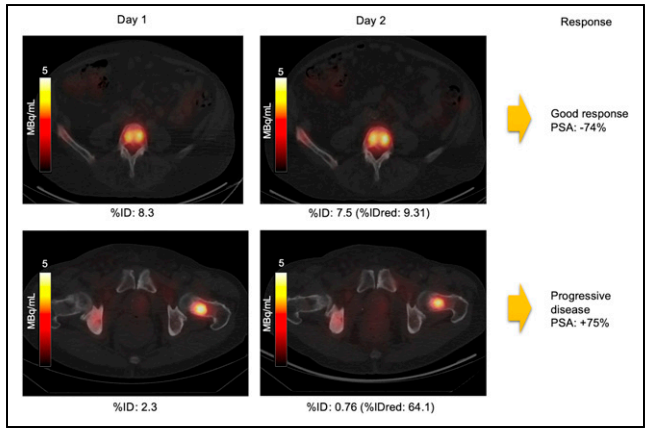

FIGURE 3. Diverging washout rate in BM lesions between case of good response (fused axial view, top panels) and one with progressive disease (fused axial view, bottom panels).

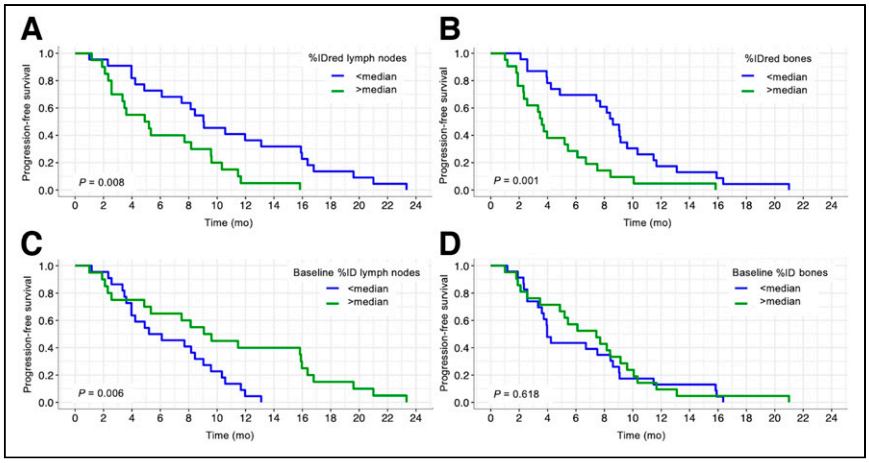

FIGURE 4. Univariable predictors of PFS. (A) LNM lesion %IDred. (B) BM lesion %IDred. (C) LNM %ID. (D) BM %ID.

1 mo after each treatment, and imaging with ^{68}Ga-PSMA-11 or ^{18}F-PSMA-1007 PET/CT had been performed 1 mo after every second RLT. Parameters related to the patients' clinical history, laboratory values, and imaging-related indices were tested; these indices were chosen on the basis of clinical reasoning and available literature data (*14*).

PFS was defined as the time elapsed between RLT start and progression; that is, 2 consecutive increases in PSA levels totaling at least 25% of the nadir (*15*), appearance of new metastatic lesions on any imaging, worsening of disease-related symptoms requiring an adjustment in supportive therapy, deterioration of general conditions, or any instance in which an mCRPC therapy change was required. OS was defined as the time between RLT start and confirmed disease-related death of the patient.

Statistical Analysis

Data are presented as median and interquartile range (IQR) unless otherwise specified. Comparisons between continuous variables between groups were made using the unpaired Student t test (2 groups) or 1-way ANOVA with least significance difference post hoc comparison (3 groups) for normally distributed data and using the Mann–Whitney test (2 groups) or Kruskal–Wallis test (3 groups) for nonnormally distributed data. Categoric variables were compared using the χ^2 or Fisher exact test, as appropriate. Correlations between continuous variables were made by means of bivariate analysis, using the Pearson coefficient. Predictors of PFS and OS were tested using the Kaplan–Meier estimator (dichotomized or categoric variables) and with a univariable Cox regression model. A multivariable model was then constructed using a combination of statistically significant image-derived and clinical parameters. The multivariable analysis was performed with the Cox proportional hazard model, and the proportional hazard assumptions were tested using Schoenfeld residuals. Multicollinearity was checked by matrix correlation. A P value of less than 0.05 was considered statistically significant.

RESULTS

Patients' Cohort Characteristics

Initially, 125 patients treated with ^{177}Lu-PSMA-617 RLT were identified. Sixty subjects were excluded because of unavailable 2–time point imaging. Five more patients were excluded who, because of mixed ^{68}Ga/^{18}F-PSMA and ^{18}F-FDG–positive disease or neuroendocrine histology, had received ^{177}Lu-PSMA-617 as a disease control attempt due to the lack of viable alternatives. Five patients were excluded because of treatment discontinuation unrelated to disease progression. Thus, 55 patients were ultimately included (Fig. 1).

Table 1 shows an overview of the 55 included patients. The subjects had a long disease history, with a median of 8.3 y between diagnosis and RLT (IQR, 3.7–14.2 y). The median time between diagnosis and mCRPC progression was 3.1 y (IQR, 1.4–9.1 y);

TABLE 2
Univariable Analysis of PFS Predictors Using Proportional Cox Regression Model

Variable	Hazard ratio	95% CI	*P*
Age	0.961	0.925–0.999	0.045
Overall disease duration	0.999	0.995–1.003	0.632
Time to mCRPC	0.997	0.992–1.002	0.29
Previous chemotherapy	0.913	0.51–1.634	0.759
Previous $^{223}RaCl_2$	0.852	0.378–1.917	0.699
More than 3 therapy lines	0.81	0.446–1.472	0.49
PSA at baseline	1	1–1.001	0.092
Hemoglobin at baseline	0.863	0.842–1.155	0.863
Tumor burden	1	1–1.001	0.6
%IDred LNM	1.026	1.011–1.042	0.001
%IDred BM	1.021	0.006–1.038	0.008
Baseline %ID LNM	0.946	0.855–1.046	0.279
Baseline %ID BM	0.983	0.953–1.015	0.29
Baseline %ID total	0.997	0.968–1.026	0.83

TABLE 3
Multivariable Analysis of PFS Predictors Using Proportional Cox Regression Model

Variable	B	SE	Wald	df	*P*	Exp(B)	95% CI
Age	−0.05	0.029	3.103	1	0.078	0.95	0.897–1.006
Time to mCRPC	0.003	0.004	0.669	1	0.413	1.003	0.995–1.012
%ID baseline LNM	0.126	0.133	0.900	1	0.343	1.134	0.874–1.472
%IDred LNM	0.020	0.009	4.717	1	0.03	1.021	1.002–1.040
%IDred BM	0.017	0.016	1.157	1	0.282	1.017	0.986–1.049

B = Beta; Wald = Wald statistics; df = degrees of freedom; Exp(B) = hazard ratio.

afterward, the patients were treated with standard approaches for a median time of 3.1 y (IQR, 2.1–4.9 y) before ^{177}Lu-PSMA-617.

On RLT start, 43 (78%), 43 (78%), or 14 (26%) subjects had LNM, BM, or organ metastasis, respectively. The latter category included liver (n = 6, 43%), lung (n = 7, 50%), and meningeal (n = 1, 7%) localizations. Subjects received a median of 3 cycles of ^{177}Lu-PSMA-617 RLT (IQR, 2–8). After the first 2 treatment cycles, 25 (45%), 12 (22%), and 18 (33%) patients were classified as responders, partial responders, and nonresponders, respectively. Tumor volume and %ID were not significantly different between responders and nonresponders.

Tracer Kinetics Across Responders and Nonresponders

Median values of %IDred within LNM were significantly higher in nonresponders (36%; IQR, 26%–47%) than in responders (24%; IQR, 12%–33%; P = 0.003; Fig. 2). When examining the variation across good, partial, and nonresponders, an increasing trend of %IDred was noted, indicating rapid tracer clearance in partial and nonresponders (partial responders, 30% [IQR, 26%–38%]; nonresponders, 42% [IQR, 33%–57%]; P = 0.001 between nonresponders and good responders; Fig. 2).

A similar pattern was detected in BM. Nonresponders had a more pronounced median %IDred drop than did responders (nonresponders, 35% [IQR, 27%–52%]; responders, 18% [IQR, 15%–29%]; P = 0.002). Partial responders had a large median %IDred overlap with nonresponders (partial responders, 28% [IQR, 23%–55%]; nonresponders, 37% [IQR, 29%–46%]; P = 0.002; Fig. 2). Figure 3 shows visual representations of the activity kinetics in BM.

In the patients' subgroup with organ metastasis, a visual and nonsignificant trend toward a difference in %IDred between responders and nonresponders could be observed (Fig. 2).

Compared with %ID, mean radioactivity concentration appeared to have at least noninferior performance in telling apart responders from nonresponders; maximum radioactivity concentration seemed to perform less well (Supplemental Table 1 [supplemental materials are available at http://jnm.snmjournals.org]).

Finally, there was a direct correlation between %IDred in LNM and %IDred in BM (R = 0.494, P = 0.005), as well as between BM and organ metastasis (R = 0.763, P = 0.006). Conversely, no correlation was found between LNM and organ metastasis (R = 0.037, P = 0.908).

Prognostic Factors of PFS

Progression occurred in all patients, with a median time to the event of 7.5 mo (95% CI, 4.7–10.3 mo). An %IDred value above the median in both LNM and BM was associated with shorter survival (Fig. 3). Moreover, higher %ID within the LNM correlated with longer survival (Fig. 4). The kinetics of ^{177}Lu-PSMA-617 within the organ metastasis had no prognostic implications (data not shown).

Supplemental Table 2 and Table 2 present an overview of all tested PFS predictors in the Kaplan–Meier and simple proportional Cox regression analyses, respectively. In the multivariable Cox regression analysis, which consisted of all factors showing a significant association with PFS in the univariable tests, only %IDred in the LNM retained a significant association with PFS (Table 3).

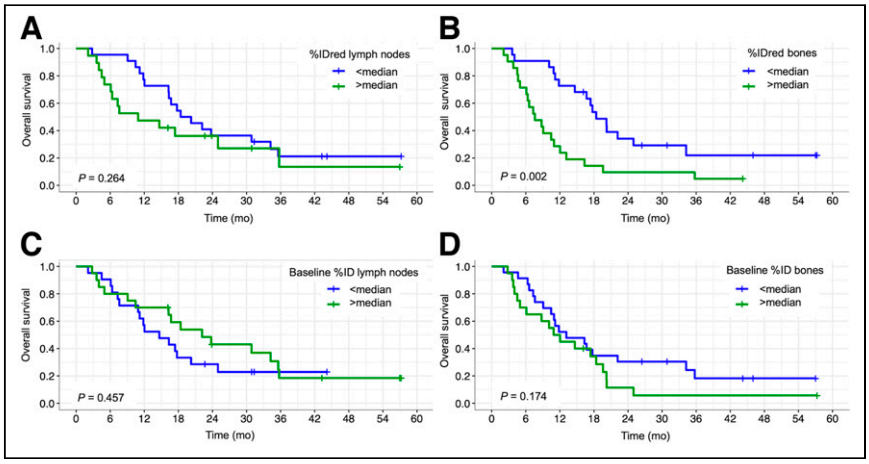

FIGURE 5. Univariable predictors of OS. (A) LNM lesion %IDred. (B) BM lesion %IDred. (C) LNM %ID. (D) BM %ID.

Prognostic Factors of OS

Forty-three patients died of disease. OS from the RLT start was 16.3 mo (95% CI, 11.1–21.6). %IDred in BM predicted OS, but neither LNM nor BM %ID was associated with OS (Fig. 5).

All tested factors in Kaplan–Meier and univariable Cox regression are presented in Supplemental Table 3 and Table 4, respectively.

In the multivariable Cox regression analysis, indices of tumor burden, as well as

TABLE 4
Univariable Analysis of OS Predictors Using Proportional Cox Regression Model

Variable	Hazard ratio	95% CI	*P*
Age	1.008	0.968–1.051	0.686
Overall disease duration	0.996	0.992–1.001	0.102
Time to mCRPC	0.998	0.992–1.003	0.422
Previous chemotherapy	0.851	0.437–1.657	0.636
Previous $^{223}RaCl_2$	0.875	0.362–2.115	0.767
More than 3 therapy lines	1.04	0.531–2.036	0.91
PSA at baseline	1.001	1–1.001	0.009
Hemoglobin at baseline	0.792	0.652–0.964	0.02
Tumor burden	1.001	1–1.001	0.021
%IDred LNM	1.017	0.997–1.037	0.089
%IDred BM	1.018	1.002–1.035	0.032
Baseline %ID LNM	1.024	0.93–1.128	0.627
Baseline %ID BM	1.001	0.971–1.033	0.971
Baseline %ID total	1.023	0.996–1.052	0.098

the degree of %IDred in BM, were associated with a worse outcome; in contrast, baseline activity within the BM lesion reduced the risk (Table 5). Similar results were obtained using the %ID total instead of the BM-specific one (Supplemental Table 4).

DISCUSSION

This study presents evidence of a prognostic role of a kinetics analysis of posttherapy images in patients treated with ^{177}Lu-PSMA-617 RLT. In particular, our data show that assessment of 2 time points of radiopharmaceutical distribution can reveal diverging patterns of uptake and washout from prostate cancer cells. Patients who will respond to the treatment show ^{177}Lu-PSMA-617 activity remaining stable or undergoing a moderate drop from the first to the second observation point. Conversely, nonresponders show more significant activity reduction within the metastases. Finally, the activity drop between the 2 time points appears to be a strong and independent prognostic marker of both PFS and OS.

The kinetics analysis suggests that a more significant drop in activity could be linked with faster tracer washout from the cells and therefore with a shorter radiopharmaceutical residence time, which could entail a smaller delivered dose to the target lesions. Conversely, stable radioactivity concentration indices could signal a longer residence time of ^{177}Lu-PSMA, resulting in a higher delivered dose and better RLT effectiveness. This hypothesis is supported by the correlation between the uptake variation within the lesion and the long-term outcome and, more specifically, by the difference in the determinants of PFS and OS: the kinetics within the LNM was predictive of disease progression, whereas the uptake patterns within the BM metastases correlated with OS. mCRPC LNM disease can quickly escalate if left unchecked or undertreated (*16,17*). However, LNM can only rarely cause morbidity or mortality per se. Conversely, the overall burden of BM has a proven impact on skeletal function and survival (*18–20*), and failure in controlling the metastatic infiltration of the skeleton can effectively reduce patients' OS. Our data confirmed these notions, showing that tracer uptake, washout rate, and tumor load were relevant to OS.

Existing data on ^{177}Lu-PSMA-617 RLT dosimetry indicate that the radiation dose delivered to the target is key in ensuring response (*21,22*). However, in a recent systematic review, a relevant variability in tumor dose (range, 7.5–77.6 Gy) was highlighted across and within populations (*23*). Technical issues and differences in tracer uptake intensity could partly account for this variability. However, because the administered activity per cycle is fixed (7,400 MBq), and given that all lesions show adequate

TABLE 5
Multivariable Analysis of OS Predictors Using Proportional Cox Regression Model

Variable	B	SE	Wald	df	*P*	Exp(B)	95% CI
PSA at baseline	0.001	0.000	9.975	1	0.002	1.001	1–1.001
Tumor burden	0.004	0.001	12.473	1	<0.001	1.004	1.002–1.006
Hemoglobin at baseline	−0.231	0.137	2.852	1	0.091	0.793	0.606–1.038
%IDred BM	0.024	0.009	6.838	1	0.009	1.025	1.006–1.143
Baseline %ID BM	−0.225	0.059	14.804	1	<0.001	0.798	0.712–0.895

B = Beta; Wald = Wald statistics; df = degrees of freedom; Exp(B) = hazard ratio.

PSMA expression (*24*), it could be hypothesized that tracer uptake and washout kinetics could be the main determinants of dose variability.

In this study, we tested the efficacy of a dual-point tracer concentration measurement approach as a sort of dosimetry proxy. Such an approach could be implemented as a quick clinical tool to identify the kinetics pattern shortly after the first treatment administration, potentially enabling salvage in cases of accelerated ^{177}Lu-PSMA-617 washout. However, this information can be obtained only after the first treatment cycle has been administered. To overcome this limitation, further studies could be designed to transfer this concept to the pre-RLT imaging setting. Using longer–half-life PSMA tracers, such as ^{64}Cu-PSMA, would allow replication of the ^{177}Lu-PSMA-617 setting (*25,26*). Another potential approach could be represented by scanners with an ultralong axial field of view, which allows very late imaging even when using radiopharmaceuticals with a relatively short half-life, such as ^{18}F-PSMA-1007 (*27,28*).

Finally, modeling of the tracer kinetics could be used to implement tailored RLT. Specifically, the supposedly reduced residence time of the radiopharmaceutical in patients with rapid ^{177}Lu-PSMA-617 washout could be compensated by increasing the dose delivered per unit of time. This task could be accomplished by increasing the administered activity or using hard-hitting radioisotopes, such as α-emitters, in lieu of ^{177}Lu (*29,30*).

This study presents some limitations. It represents a single-center, retrospective investigation that is thereby susceptible to selection bias; strict selection criteria were used to avoid distortion. Even though we analyzed organ metastasis, we could not determine whether a difference in the tracer kinetics between responders and nonresponders exists. This limitation could result from the small sample size, as well as the heterogeneity of said metastasis, which were in different organs. Nonetheless, similarities in the washout behavior between organ metastasis and BM could be identified, as highlighted by the correlation analysis, hinting that these hallmarks of advanced disease tend to show comparable ^{177}Lu-PSMA-617 kinetics. Treatment response was always assessed after the second RLT cycle without considering the maximum potential PSA decline; this choice was made to ensure consistency, because the latter information was not always available.

Data from the pre-RLT PET/CT were available, yet the tracer uptake intensity (SUV) was not factored into the univariate and multivariate analyses, given the large variability of time elapsed between imaging and RLT and that the tracer had been changed during the observation period (^{68}Ga-PSMA-11 to ^{18}F-PSMA-1007). Considering later time points in SPECT/CT, for example, 72–120 h after injection, could have improved the prognostic power of the washout index. However, the overall goal of this research line is to identify the kinetics trends as early and with as few time points as possible to make the technique eventually feasible for everyday routine. Finally, many factors can affect OS, especially in patients with a long disease history. To ensure homogeneity and assess the impact of clinical variables on the outcome, we adopted tight selection criteria and tested each of them with a survival analysis model.

CONCLUSION

The ^{177}Lu-PSMA-617 kinetics in LNM and BM appear to be prognostic of treatment response, as well as of survival. In particular, OS appears to be linked with the kinetics parameters of BM, in keeping with the concept that BM is the most threatening pathogenic mechanism of mCRPC. This information, which should be confirmed by prospective trials, is readily obtainable from post-therapy scans and could be used to prognosticate treatment outcomes and design studies aimed to investigate the potential of PET-based prediction, as well as the possibility of patient-adapted therapeutic protocols of RLT.

DISCLOSURE

No potential conflict of interest relevant to this article was reported.

ACKNOWLEDGMENT

This work was supported by the Deutsche Forschungsgemeinschaft (German Research Foundation, Germany's Excellence Strategy, EXC2180-390900677).

KEY POINTS

QUESTION: Are the ^{177}Lu-PSMA-617 kinetics in mCRPC localizations relevant to treatment effectiveness?

PERTINENT FINDINGS: Greater reduction of ^{177}Lu-PSMA-617 concentration within metastasis over time was associated with reduced response rate and shorter survival.

IMPLICATIONS FOR PATIENT CARE: The kinetics information could be used in studies on RLT tailoring to test the effectiveness of increase of activity or the use of higher-energy isotopes in bolstering the target dose in patients with faster washout.

REFERENCES

1. Sartor O, de Bono J, Chi KN, et al. Lutetium-177-PSMA-617 for metastatic castration-resistant prostate cancer. *N Engl J Med.* 2021;385:1091–1103.
2. Hofman MS, Emmett L, Sandhu S, et al. [^{177}Lu]Lu-PSMA-617 versus cabazitaxel in patients with metastatic castration-resistant prostate cancer (TheraP): a randomised, open-label, phase 2 trial. *Lancet.* 2021;397:797–804.
3. von Eyben FE, Roviello G, Kiljunen T, et al. Third-line treatment and ^{177}Lu-PSMA radioligand therapy of metastatic castration-resistant prostate cancer: a systematic review. *Eur J Nucl Med Mol Imaging.* 2018;45:496–508.
4. Yadav MP, Ballal S, Sahoo RK, Dwivedi SN, Bal C. Radioligand therapy with ^{177}Lu-PSMA for metastatic castration-resistant prostate cancer: a systematic review and meta-analysis. *AJR.* 2019;213:275–285.
5. Kim YJ, Kim Y-I. Therapeutic responses and survival effects of ^{177}Lu-PSMA-617 radioligand therapy in metastatic castrate-resistant prostate cancer: a meta-analysis. *Clin Nucl Med.* 2018;43:728–734.
6. Sartor O, de Bono J, Chi KN, et al. Lutetium-177-PSMA-617 for metastatic castration-resistant prostate cancer. *N Engl J Med.* 2021;385:1091–1103.
7. Has Simsek D, Kuyumcu S, Karadogan S, et al. Outcome of ^{177}Lu-PSMA radionuclide treatment in advanced prostate cancer and its association with clinical parameters: a single-center experience. *Clin Nucl Med.* 2022;47:e521–e528.
8. Calais J, Czernin J. PSMA expression assessed by PET imaging is a required biomarker for selecting patients for any PSMA-targeted therapy. *J Nucl Med.* 2021; 62:1489–1491.
9. Wester HJ, Schottelius M. PSMA-targeted radiopharmaceuticals for imaging and therapy. *Semin Nucl Med.* 2019;49:302–312.
10. Violet J, Jackson P, Ferdinandus J, et al. Dosimetry of ^{177}Lu-PSMA-617 in metastatic castration-resistant prostate cancer: correlations between pretherapeutic imaging and whole-body tumor dosimetry with treatment outcomes. *J Nucl Med.* 2019; 60:517–523.
11. Michalski K, Ruf J, Goetz C, et al. Prognostic implications of dual tracer PET/CT: PSMA ligand and [^{18}F]FDG PET/CT in patients undergoing [^{177}Lu]PSMA radioligand therapy. *Eur J Nucl Med Mol Imaging.* 2021;48:2024–2030.
12. Lee WW. Clinical applications of technetium-99m quantitative single-photon emission computed tomography/computed tomography. *Nucl Med Mol Imaging.* 2019; 53:172–181.

13. Dorbala S, Park MA, Cuddy S, et al. Absolute quantitation of cardiac ^{99m}Tc-pyrophosphate using cadmium-zinc-telluride-based SPECT/CT. *J Nucl Med.* 2021;62:716–722.
14. Gafita A, Calais J, Grogan TR, et al. Nomograms to predict outcomes after ^{177}Lu-PSMA therapy in men with metastatic castration-resistant prostate cancer: an international, multicentre, retrospective study. *Lancet Oncol.* 2021;22:1115–1125.
15. Scher HI, Morris MJ, Stadler WM, et al. Trial design and objectives for castration-resistant prostate cancer: updated recommendations from the prostate cancer clinical trials working group 3. *J Clin Oncol.* 2016;34:1402–1418.
16. Klusa D, Lohaus F, Furesi G, et al. Metastatic spread in prostate cancer patients influencing radiotherapy response. *Front Oncol.* 2021;10:627379.
17. Fleischmann A, Schobinger S, Schumacher M, Thalmann GN, Studer UE. Survival in surgically treated, nodal positive prostate cancer patients is predicted by histopathological characteristics of the primary tumor and its lymph node metastases. *Prostate.* 2009;69:352–362.
18. Dittmann H, Kaltenbach S, Weissinger M, et al. The prognostic value of quantitative bone SPECT/CT before ^{223}Ra treatment in metastatic castration-resistant prostate cancer. *J Nucl Med.* 2021;62:48–54.
19. Fiz F, Dittman H, Campi C, et al. Assessment of skeletal tumor load in metastasized castration-resistant prostate cancer patients: a review of available methods and an overview on future perspectives. *Bioengineering (Basel).* 2018;5:1–13.
20. Fiz F, Sahbai S, Campi C, et al. Tumor burden and intraosseous metabolic activity as predictors of bone marrow failure during radioisotope therapy in metastasized prostate cancer patients. *BioMed Res Int.* 2017;2017:3905216.
21. Violet J, Jackson P, Ferdinandus J, et al. Dosimetry of ^{177}Lu-PSMA-617 in metastatic castration-resistant prostate cancer: correlations between pretherapeutic imaging and whole-body tumor dosimetry with treatment outcomes. *J Nucl Med.* 2019;60:517–523.
22. Götz TI, Lang EW, Prante O, et al. Estimation of [^{177}Lu]PSMA-617 tumor uptake based on voxel-wise 3D Monte Carlo tumor dosimetry in patients with metastasized castration resistant prostate cancer. *Nuklearmedizin.* 2020;59:365–374.
23. Nautiyal A, Jha AK, Mithun S, Rangarajan V. Dosimetry in Lu-177-PSMA-617 prostate-specific membrane antigen targeted radioligand therapy: a systematic review. *Nucl Med Commun.* 2022;43:369–377.
24. Kratochwil C, Fendler WP, Eiber M, et al. EANM procedure guidelines for radionuclide therapy with ^{177}Lu-labelled PSMA-ligands (^{177}Lu-PSMA-RLT). *Eur J Nucl Med Mol Imaging.* 2019;46:2536–2544.
25. Lee C-H, Lim I, Woo S-K, et al. The feasibility of ^{64}Cu-PSMA I&T PET for prostate cancer. *Cancer Biother Radiopharm.* 2022;37:417–423.
26. Liu T, Liu C, Zhang Z, et al. ^{64}Cu-PSMA-BCH: a new radiotracer for delayed PET imaging of prostate cancer. *Eur J Nucl Med Mol Imaging.* 2021;48:4508–4516.
27. Spencer BA, Berg E, Schmall JP, et al. Performance evaluation of the uEXPLORER total-body PET/CT scanner based on NEMA NU 2-2018 with additional tests to characterize long axial field-of-view PET scanners. *J Nucl Med.* 2021;62:861–870.
28. Badawi RD, Shi H, Hu P, et al. First human imaging studies with the EXPLORER total-body PET scanner. *J Nucl Med.* 2019;60:299–303.
29. Kratochwil C, Bruchertseifer F, Giesel FL, et al. ^{225}Ac-PSMA-617 for PSMA-targeted α-radiation therapy of metastatic castration-resistant prostate cancer. *J Nucl Med.* 2016;57:1941–1944.
30. Zacherl MJ, Gildehaus FJ, Mittlmeier L, et al. First clinical results for PSMA-targeted α-therapy using ^{225}Ac-PSMA-I&T in advanced-mCRPC patients. *J Nucl Med.* 2021;62:669–674.